Palladium-Catalyzed Asymmetric Allylic Amination Using Ferrocenyl Pyrazole Ligands: Steric Control of η^3-Allyl Configuration and Site-Selective Nucleophilic Attack

Antonio Togni,*,† Urs Burckhardt,† Volker Gramlich,‡ Paul. S. Pregosin,† and Renzo Salzmann†

Contribution from the Laboratory of Inorganic Chemistry and Institute of Crystallography and Petrography, Swiss Federal Institute of Technology, ETH-Zentrum, CH-8092 Zürich, Switzerland

Received September 5, 1995[⊗]

Abstract: The reaction of 1,3-diphenylallylethyl carbonate (**1**) with benzylamine to afford the secondary amine **2** is effectively catalyzed by Pd-complexes containing chiral ferrocenyl pyrazole ligands. The highest enantioselectivity (99% ee) was obtained using ligand **3a**, 1-{(*S*)-1-[(*R*)-2-(diphenylphosphino)ferrocenyl]ethyl}-3-(1-adamantyl)-1*H*-pyrazole. Four different cationic Pd-allyl intermediates, **4a**, **4c**, **4j**, and **4k** (containing ligands **3a**, **3c**, **3j**, and **3k**, respectively), formed during the catalytic reaction were studied in solution by 2D-NMR spectroscopy, with the aim of clarifying configurational aspects. Depending on the size and shape of the substituent in position 3 of the pyrazole ring, it was found that the major diastereoisomeric form of these complexes either adopts an *exo-syn-syn* (ligands **3a** and **3c**, 1-{(*S*)-1-[(*R*)-2-(diphenylphosphino)ferrocenyl]-ethyl}-3-phenyl-5-methyl-1*H*-pyrazole) or an *exo-syn-anti* configuration (ligands **3j**, 1-{(*S*)-1-[(*R*)-2-(diphenylphosphino)ferrocenyl]ethyl}-3-(9-anthryl)-5-methyl-1*H*-pyrazole and **3k**, 1-{(*S*)-1-[(*R*)-2-(diphenylphosphino)ferrocenyl]ethyl}-3-(9-triptycyl)-1*H*-pyrazole). This analysis allows the site of nucleophilic attack on the allyl ligand to be established unequivocally, i.e., the carbon atom trans to phosphorus. The reasons responsible for this pronounced site-selectivity are discussed. The Pd-allyl complexes [Pd(η^3-PhCHCHCHPh)(**3c**)]PF_6, **4c**, and [Pd(η^3-PhCHCHCHPh)(**3k**)]PF_6, **4k**, were characterized by X-ray diffraction. **4c** crystallizes with 1 equiv of Et_2O in the orthorhombic space group $P2_12_12_1$: $a = 13.026(2)$ Å, $b = 14.784(2)$ Å, $c = 25.124(5)$ Å, $Z = 4$. Crystals of **4k** contain 3 equiv of hexane and 1 equiv of acetone and H_2O in the unit cell belonging to the trigonal system, space group $P3_221$: $a = 24.07(3)$ Å, $c = 22.48(3)$ Å, $Z = 6$.

Introduction

Enantioselective palladium-catalyzed substitution reactions of allylic substrates[1] have received a new impetus in recent years thanks to the development of novel chiral chelating ligands. Thus, nitrogen-containing auxiliaries,[2] in particular, have been shown to belong to the most effective chiral inducing agents for reactions of allylic acetates or carbonates with soft carbon nucleophiles.[3] Assuming that the chiral ligands lack any element of symmetry, plus symmetrically substituted allylic substrates, the enantioselectivity observed will depend upon three main factors: (1) the relative concentrations of the different possible configurational isomers of the Pd(η^3-allyl) complexes present as intermediates (see Chart 1), (2) their relative rates of reaction with the nucleophile, and (3) the site of nucleophilic attack at the inequivalent allylic positions 1 and 3.

Concomitant with the successful development of new ligands, affording enantioselectivities as high as 99% ee for the reaction of 1,3-diphenylallyl acetate with dimethyl malonate, studies addressing the subtle aspects concerning the origin of enantioselectivity have been reported recently. For the P,N-ligand systems developed by Pfaltz and Helmchen[3e] and Brown[3k] it is generally agreed that the nucleophilic attack takes place preferentially at the allyl terminus trans to phosphorus.[4] However, uncertainty still exists concerning the profound reasons leading to such a site-selectivity.[5] Despite its inherent

Chart 1

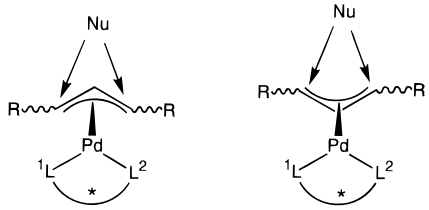

† Laboratory of Inorganic Chemistry.

‡ Institute of Crystallography and Petrography.

[⊗] Abstract published in *Advance ACS Abstracts,* January 1, 1996.

(1) For reviews, see: (a) Consiglio, G.; Waymouth, R. M. *Chem. Rev.* **1989**, *89*, 257−276. (b) Hayashi, T. In *Catalytic Asymmetric Synthesis*; Ojima, I., Ed.; VCH: New York, 1993; pp 325−365. (c) Godleski, S. A. In *Comprehensive Organic Synthesis*; Trost, B. M., Fleming, I., Eds.; Pergamon: Oxford, 1991; Vol. 4, Chapter 3.3, pp 585−661. (d) Frost, C. G.; Howarth, J.; Williams, J. M. J. *Tetrahedron: Asymmetry* **1992**, *3*, 1089−1122.

(2) For a recent review, see: Togni, A.; Venanzi, L. M. *Angew. Chem., Int. Ed. Engl.* **1994**, *33*, 497−526 (*Angew. Chem.* **1994**, *106*, 517−548).

(3) For recent pertinent examples, see: (a) Leutenegger, U.; Umbricht, G.; Fahrni, C.; von Matt, P.; Pfaltz, A. *Tetrahedron* **1992**, *48*, 2143−2156. (b) von Matt, P.; Pfaltz, A. *Angew. Chem., Int. Ed. Engl.* **1993**, *32*, 566 (*Angew. Chem.* **1993**, *105*, 614). (c) von Matt, P.; Loiseleur, O.; Koch, G.; Pfaltz, A.; Lefeber, C.; Feucht, T.; Helmchen, G. *Tetrahedron: Asymmetry* **1994**, *5*, 573. (d) Sprinz, J.; Helmchen, G. *Tetrahedron Lett.* **1993**, *34*, 1769−1772. (e) Sprinz, J.; Kiefer, M.; Helmchen, G.; Reggelin, M.; Huttner, G.; Walter, O.; Zsolnai, L. *Tetrahedron Lett.* **1994**, *35*, 1523−1526. (f) Frost, C. G.; Williams, J. M. J. *Tetrahedron Lett.* **1993**, *34*, 2015−2018. (g) Dawson, G. J.; Frost, C. G.; Williams, J. M. J.; Coote, S. J. *Tetrahedron Lett.* **1993**, *34*, 7793−7796. (h) Frost, C. G.; Williams, J. M. J. *Tetrahedron: Asymmetry* **1993**, *4*, 1785−1788. (i) Bovens, M.; Togni, A.; Venanzi, L. M. *J. Organomet. Chem.* **1993**, *451*, C28-C31. (j) Kubota, H.; Nakajima, M.; Koga, K. *Tetrahedron Lett.* **1993**, *34*, 8135−8138. (k) Brown, J. M.; Hulmes, D. I.; Guiry, P. J. *Tetrahedron* **1994**, *50*, 4493−4506. (l) Brenchley, G.; Merifield, E.; Wills, M.; Fedouloff, M. *Tetrahedron Lett.* **1994**, *35*, 2791−2794. (m) Tanner, D.; Andersson, P. G.; Harden, A.; Somfai, P. *Tetrahedron Lett.* **1994**, *35*, 4631−4634. (n) Gamez, P.; Dunjic, B.; Fache, M.; Lemaire, M. *J. Chem. Soc. Chem. Commun.* **1994**, 1417−1418. (o) Kang, J.; Cho, W. O.; Cho, H. G. *Tetrahedron: Asymmetry* **1994**, *5*, 1347−1352. (p) von Matt, P.; Lloyd-Jones, G. C.; Minidis, A. B. E.; Pfaltz, A.; Macko, L.; Neuburger, M.; Zehnder, M.; Rüegger, H.; Pregosin, P. S. *Helv. Chim. Acta* **1995**, *78*, 265−284.

0002-7863/96/1518-1031$12.00/0

Scheme 1

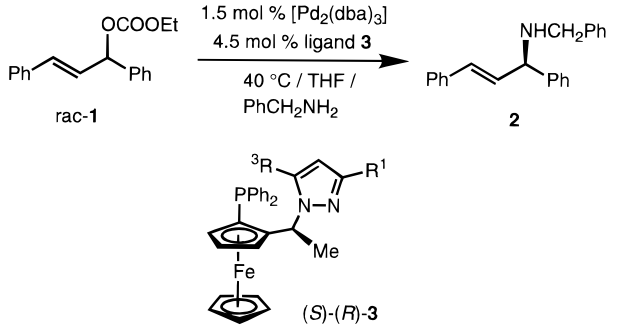

interest, we note that less attention has been devoted to the analogous transformations involving amines as the nucleophilic component.[6]

We recently reported the successful application of pyrazole-containing ferrocenyl phosphines (P,N-ligands) of type **3**[7] in the Rh-catalyzed hydroboration of styrene with catecholborane affording enantioselectivities up to 98% ee. These encouraging results prompted us to extend the scope of these ligands to the model reaction of racemic 1,3-diphenylallylethyl carbonate (**1**) with benzylamine, reported here and illustrated in Scheme 1. The focus of our study is thereby more mechanistic than synthetic in nature and on these lines we present evidence that the nucleophilic attack occurs, not unexpectedly, preferentially at the allylic terminus trans to the phosphine moiety. Furthermore, and more importantly, we show that the configuration of the Pd(η^3-allyl) intermediate can effectively be controlled by the steric nature of the ligand, this aspect providing an unprecedented mechanistic tool.

Results and Discussion

Reactions of carbonate **1** with benzylamine were carried out in THF at 40 °C in the presence of 1.5 mol % of $[Pd_2(dba)_3]\cdot CHCl_3$ as a catalyst precursor and 4.5 mol % of the corresponding pyrazole ligand (*S*)-(*R*)-**3**.[8] After a typical reaction time of 12 h, the amination product (*R*)-**2**[9] was isolated after chromatographic purification in 90−95% yield. A brief screening of the available pyrazole ligands **3**[7b] indicated that a sterically relatively large substituent is needed at position 3 of the heterocycle, in order to obtain enantioselectivities in the range of 94−99 % ee. A collection of selectivity data as a function of the ligand used is given in Table 1. Thus, several aryl substituents are well tolerated as well as the relatively bulky cyclohexyl group (ligands **3b**−**i**). The very rigid, compact, and large substituent 1-adamantyl (ligand **3a**) was found to afford the unprecedented value of 99% ee for this reaction. Ligand **3l** containing the less bulky methyl group at position 3 gives a significantly lower stereoselectivity (90% ee).

Table 1. Enantioselectivities Observed for the Reaction of Scheme 1 as a Function of the Ligand Used

ligand[a]	R^1	R^2	% ee[b] (abs. conf.)
(*S*)-(*R*)-**3a**	1-adamantyl	H	99 (*R*)
(*S*)-(*R*)-**3b**	cyclohexyl	Me	95 (*R*)
(*S*)-(*R*)-**3c**	Ph	Me	96 (*R*)
(*S*)-(*R*)-**3d**	Ph	H	95 (*R*)
(*S*)-(*R*)-**3e**	1-naphthyl	Me	94 (*R*)
(*S*)-(*R*)-**3f**	2-naphthyl	Me	94 (*R*)
(*S*)-(*R*)-**3g**	4-pyridinyl	Me	96 (*R*)
(*S*)-(*R*)-**3h**	3-NO_2-Ph	H	97 (*R*)
(*S*)-(*R*)-**3i**	2,4$(MeO)_2$Ph	Me	95 (*R*)
(*S*)-(*R*)-**3j**	9-anthryl	Me	40 (*S*)
(*S*)-(*R*)-**3k**	9-triptycyl	H	no reaction
(*S*)-(*R*)-**3l**	Me	Me	90 (*R*)

[a] Control reactions were also performed with the (*R*)-(*S*)-enantiomers of the ligands. [b] Determined by HPLC (see Experimental Section).

Much to our surprise, the reaction involving the analogous ligand (*S*)-(*R*)-**3j** containing a 9-anthryl substituent gave the (*S*)-**2** product in only 40% ee under the same conditions. This drastic change (inversion) of enantioselectivity can only be due to a major steric influence of the new substituent on the configuration of the Pd(η^3-allyl) intermediate and/or on the site of nucleophilic attack, since the absolute configuration of the ligand is constant, and no significantly different electronic effects are anticipated.[10] In order to understand this unexpected observation, we decided to study the structure of the corresponding cationic Pd(η^3-1,3-diphenylallyl) complexes (1) in the solid state by X-ray diffraction and (2) in solution by 2D NMR spectroscopy.[11] This kind of intermediate in the catalytic reaction is easily accessible in crystalline form from the dinuclear compound $[Pd_2(\eta^3\text{-}1,3\text{-diphenylallyl})_2Cl_2]$,[6a] the chelating ligand, and a chloride scavenging agent, such as $TlPF_6$.

Thus, the crystal and molecular structure of the compound [Pd(η^3-1,3-diphenylallyl)((*S*)-(*R*)-**3c**)]PF_6 (**4c**) clearly shows the allyl ligand in an *exo-syn-syn* configuration (*exo* refers to the relative orientation of the central allylic C−H vector pointing away from the ferrocene core), as it is apparent from the ORTEP view of Figure 1. Table 2 collects a selection of bond lengths and angles. The structure turns out to be rather routine, with a pseudo square planar geometry around palladium, and all bonding parameters falling in the expected ranges.[12] However,

(4) The reported studies base their conclusion upon the analysis of the structures both in solution and in the solid state of Pd-allyl intermediates. They correlate the configuration of the major isomer of the η^3-allyl intermediate with the absolute configuration of the product. This is a typical ground-state argument, as it has been previously put forward by Bosnich; see: (a) Auburn, P. R.; Mackenzie, P. B.; Bosnich, B. *J. Am. Chem. Soc.* **1985**, *107*, 2033−2046. (b) Mackenzie, P. B.; Whelan, J.; Bosnich, B. *J. Am. Chem. Soc.* **1985**, *107*, 2046−2054. An alternative way of directing the incoming nucleophile by means of secondary interactions with a functional group contained in the ligands has been developed by Hayashi and Ito. For a review, see: Sawamura, M.; Ito, Y. *Chem. Rev.* **1992**, *92*, 857−871, and references cited therein.

(5) Helmchen[3e] pointed out the importance of an early transition state, whereas Brown[3k] indicated the significance of repulsive steric interactions in a late transition state.

(6) For successful approaches utilizing 1,3-disubstituted acyclic allylic substrates, see: (a) Hayashi, T.; Yamamoto, A.; Ito, Y.; Nishioka, E.; Miura, H.; Yanagi, K. *J. Am. Chem. Soc.* **1989**, *111*, 6301−6311. (b) Hayashi, T.; Kishi, K.; Yamamoto, A.; Ito, Y. *Tetrahedron Lett.* **1990**, *31*, 1743−1746. (c) Hayashi, T.; Yamamoto, A.; Ito, Y. *Tetrahedron Lett.* **1988**, *29*, 99−102. (d) von Matt, P.; Loiseleur, O.; Koch, G.; Pfaltz, A.; Lefeber, C.; Feucht, T.; Helmchen, G. *Tetrahedron: Asymmetry* **1994**, *5*, 573−584. Furthermore, Trost and co-workers developed the amination of cyclic allylic substrates, based on the enantiotopic group differentiation. See: (e) Trost, B. M.; Van Vranken, D. L.; Bingel, C. *Angew. Chem., Int. Ed. Engl.* **1992**, *31*, 228−229 (*Angew. Chem.* **1992**, *104*, 194−196). (f) Trost, B. M.; Van Vranken, D. L.; Bingel, C. *J. Am. Chem. Soc.* **1992**, *114*, 9327−9343. (g) Trost, B. M.; Van Vranken, D. L. *J. Am. Chem. Soc.* **1993**, *115*, 444−458.

(7) (a) Schnyder, A.; Hintermann, L.; Togni, A. *Angew. Chem., Int. Ed. Engl.* **1995**, *34*, 931−933 (*Angew. Chem.* **1995**, *107*, 996−998). (b) Burckhardt, U.; Hintermann, L.; Schnyder, A.; Togni, A. *Organometallics* **1995**, *14*, 5415−5425.

(8) These reaction conditions correspond to those reported by Hayashi and co-workers, see ref 6a.

(9) Assignment of the absolute configuration has been made by comparing the sign of the optical rotation with that reported in the literature (ref 6a).

(10) For the observation of important electronic effects on stereoselectivity using this kind of ligands, see ref 7a.

(11) A detailed account on the characterization and comparison of the structural features in solution, as obtained by 2D-NMR methods, is in preparation.

(12) (a) Orpen, A. G.; Brammer, L.; Allen, F. H.; Kennard, O.; Watson, D. G.; Taylor, R. *J. Chem. Soc., Dalton Trans.* **1989**, Supplement S1−S83. (b) Allen, F. H.; Kennard, O.; Watson, D. G.; Brammer, L.; Orpen, A. G.; Taylor, R. *J. Chem. Soc., Perkin Trans II* **1987**, Supplement S1−S19.

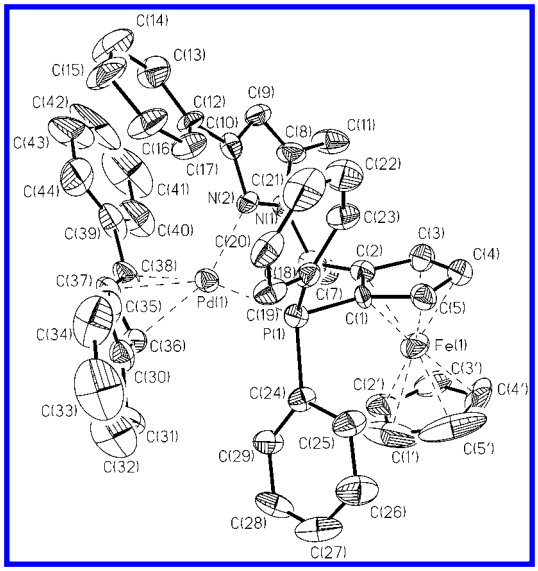

Figure 1. ORTEP view (30% ellipsoids) and atom numbering scheme for the cation (*S*)-(*R*)-**4c**.

Table 2. Selected Bond Distances (Å)[a] and Angles (deg)[a] for (*S*)-(*R*)-**4c** and (*R*)-(*S*)-**4k**

(*S*)-(*R*)-**4c**		(*R*)-(*S*)-**4k**	
	Bond Distances		
Pd−P	2.321(4)	Pd−P	2.344(7)
Pd−N(2)	2.131(11)	Pd−N(2)	2.225(15)
Pd−C(36)	2.138(16)	Pd−C(43)	2.161(18)
Pd−C(37)	2.173(16)	Pd−C(44)	2.064(24)
Pd−C(38)	2.268(13)	Pd−C(45)	2.213(19)
C(36)−C(37)	1.436(22)	C(43)−C(44)	1.391(35)
C(37)−C(38)	1.380(23)	C(44)−C(45)	1.369(31)
N(1)−N(2)	1.359(17)	N(1)−N(2)	1.342(34)
	Bond Angles		
P−Pd−N(2)	95.0(3)	P−Pd−N(2)	101.3(5)
N(2)−Pd−C(38)	94.5(5)	N(2)−Pd−C(45)	97.0(7)
P−Pd−C(36)	105.3(4)	P−Pd−C(43)	97.3(5)
C(36)−C(37)−C(38)	121.0(16)	C(43)−C(44)−C(45)	115.8(27)
C(30)−C(36)−C(37)	122.4(15)	C(44)−C(43)−C(46)	124.3(23)
C(37)−C(38)−C(39)	126.0(19)	C(44)−C(45)−C(52)	135.9(23)

[a] Number in parentheses are esd's in the least significant digits.

several characteristics are worth noting. Thus, the conformation of the ligand qualitatively corresponds to that found for free ligands of type **3**,[7b] with the pyrazole fragment in a pseudo axial position. The phenyl group on the allyl carbon trans to nitrogen intrudes into the region between the two phenyl rings on phosphorus. This arrangement could rationalize the preference for the *exo* orientation of the allyl ligand. The Pd−C bond lengths are significantly different from one another, the carbon atom trans to phosphorus displaying the expected longer distance (Pd−C(38) = 2.268(13) Å), as compared to its partner trans to nitrogen (Pd−C(36) = 2.138(16) Å). This is an expression of the higher trans influence[13] of the phosphine ligand. The plane of the allyl ligand is tilted 32.6° from the perpendicular to the Pd−N−P plane, and the latter forms an angle of 36.0° with the "upper" Cp ring. In view of the overall mechanistic discussion (vide infra), an important distorsion of the Pd-allyl fragment is observed. The allyl ligand, with respect to its idealized orientation, is rotated in an anti-clockwise manner around the Pd-allyl axis, as seen from the π-ligand toward the Pd atom (for the (*S*)-(*R*) absolute configuration of the ferrocenyl moiety). This is reflected, e.g., by two very different interplanar angles that should be identical in the case of an ideal geometry. Indeed,

(13) For a review see, e.g.: Appleton, T. G.; Clark, H. C.; Manzer, L. E. *Coord. Chem. Rev.* **1973**, *10*, 335−422.

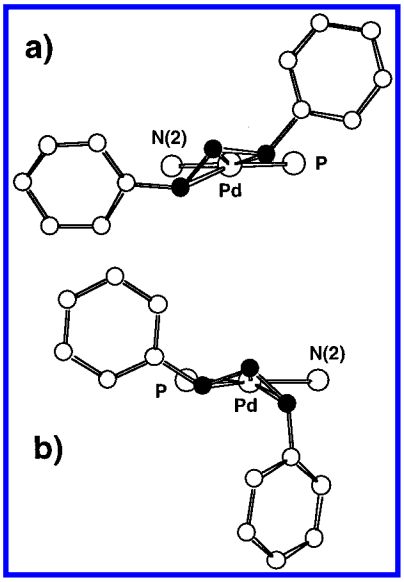

Figure 2. Projections of the allyl ligands of compounds (*S*)-(*R*)-**4c** (a)) and (*R*)-(*S*)-**4k** (b)) along the Pd−P−N(2) plane.

the angles formed by the Pd−P−N(2) plane and the planes defined by Pd, C(36), and C(37) and Pd, C(37), and C(38) are 11.8° and 46.5°, respectively. This means that the unit C(37)−C(36) (trans to nitrogen) is already almost coplanar with the atoms Pd, P, and N(2), as schematically illustrated in Figure 2a.

^{31}P, ^{13}C, and ^{1}H spectra (selected data are presented in Table 3), and specifically a 2D ^{1}H NOESY spectrum[14] of complex **4c** (see Figure 3a) measured in THF-d_8 at 40 °C, to reflect the reaction medium used for the catalytic experiments, confirmed that the major isomer (85%) observed in solution had the same structure shown in the solid state. However, of the three remaining isomers two could be identified, i.e., the *endo-syn-syn* form (6%) and the *endo-syn-anti* form (6%). The latter is exchanging with the major isomer,[15] and has the *anti* phenyl on the allyl carbon atom in pseudo trans position with respect to the pyrazole moiety. The structure of the fourth isomer (3%) could not be assigned unequivocally. The assignment of the allyl configuration is based on (1) ^{1}H spin−spin coupling constants and classical intra-allyl NOEs (it is worth remembering that a strong NOE between the central allylic proton and just one of the two terminal protons indicates a *syn-anti* arrangement), (2) an NOE between the central allyl proton and *ortho* protons on the phenyl group attached to the pyrazole determines the *exo* configuration, and (3) NOEs between the *anti* terminal allyl proton and the *ortho* protons of the phenyl group on the pyrazole. Note that the absence of such an NOE involving the central allyl proton, indicates the *endo* orientation.

Under the assumption that the observed major enantiomer of the product (absolute configuration *R*) of the catalytic reaction reflects preferential nucleophilic attack on the major *exo-syn-syn* isomer, then a correlation between the observed absolute configuration and the site of nucleophilic attack is possible. Such a correlation indicates *preferential attack at the allylic carbon atom trans to phosphorus*. However, it is important to realize

(14) For details concerning the application of NOESY spectroscopy to the structural characterization of Pd-allyl complexes in solution, see, e.g.: (a) Pregosin, P. S.; Salzmann, R.; Togni, A. *Organometallics* **1995**, *14*, 842−847. (b) Abbenhuis, H. C. L.; Burckhardt, U.; Gramlich, V.; Köllner, C.; Pregosin, P. S.; Salzmann, R.; Togni, A. *Organometallics* **1995**, *14*, 759−766, and pertinent references cited therein.

(15) A section of the phase-sensitive NOESY spectrum showing this particular selective exchange occuring on the NMR time scale is provided as supporting information. A simple $\pi-\sigma-\pi$ equilibrium could account for this interconversion.

Table 3. Selected 500 MHz ^{1}H, 125.8 MHz ^{13}C, and 202.6 MHz ^{31}P NMR data (d_8-THF) for compounds **4a**, **4c**, **4j**, and **4k**

	compound						
	exo-syn-syn-**4a**	*exo-syn-syn*-**4c**	*endo-syn-anti*-**4c**	*endo-syn-syn*-**4c**	*exo-syn-anti*-**4j**	*exo-syn-syn*-**4j**	*exo-syn-anti*-**4k**
	11.8[b]	14.2[b]	12.0[b]	13.4[b]	12.0[b]	8.2[b]	11.4[b]
	δ^1H (δ^{13}C)	δ^1H (δ^{13}C)	δ^1H (δ^{13}C)	δ^1H (δ^{13}C)	δ^1H (δ^{13}C)	δ^1H (δ^{13}C)	δ^1H (δ^{13}C)
CH(1)[c]	7.26 (107.9)	6.43 (104.4)	5.57 (95.0)	4.50 (93.0)	5.18 (102.4)	7.40 (115.1)	5.41 (98.7)
CH(2)	6.49 (113.8)	5.94 (111.5)	6.54 (106.7)	6.92 (108.7)	3.63 (106.5)	5.18 (107.0)	3.98 (105.5)
CH(3)	5.34 (65.9)	5.15 (67.9)	6.67 (75.9)	5.10 (79.5)	5.43 (71.3)	4.64 (67.8)	4.81 (75.3)
CH(4)	2.37 (18.0)	2.35 (18.5)	1.84 (17.3)	2.03 (17.6)	2.37 (17.4)	2.52 (19.2)	2.45 (20.3)
CH(5)	7.08 (59.1)	6.85 (60.4)	6.32 (60.1)	6.53 (60.3)	6.12 (59.8)	7.49 (60.1)	6.54 (58.5)
CH(6)	4.07 (73.7)	4.05 (73.7)	3.99[a]	4.02[a]	3.93 (74.6)	4.28 (74.1)	4.34(73.6)
CH(7)	4.46 (71.3)	4.56 (72.0)	4.59[a]	4.53[a]	4.68 (71.6)	4.68(70.8)	4.53 (70.6)
CH(8)	4.72 (67.0)	4.80 (67.1)	4.82[a]	4.77[a]	5.36 (70.4)	5.18 (67.4)	5.02 (67.6)
CH(9)	6.00 (106.4)	5.93 (109.3)	*a*	*a*	6.64 (113.5)	6.29 (115.6)	7.37 (113.9)
CH(10)	7.85 (130.0)	2.46 (13.0)	2.23 (12.6)	2.29 (12.9)	2.79 (12.0)	2.77 (12.3)	8.65 (131.2)
η^5-C_5H_5	3.95 (71.8)	3.95 (71.4)	*a*	*a*	3.80 (71.5)	4.05 (72.1)	3.47 (71.0)

[a] Resonance could not be unequivocally assigned. [b] δ^{31}P. [c] Arbitrary atom numbering scheme:

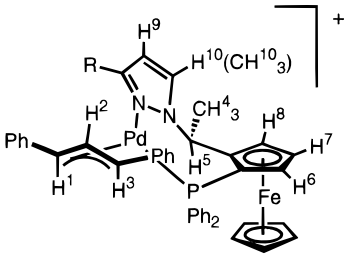

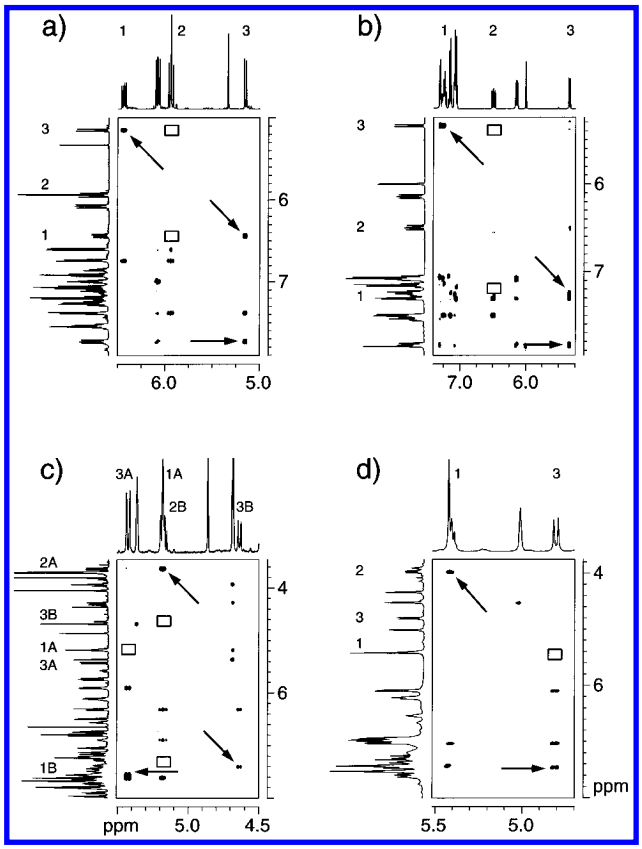

Figure 3. Sections of the phase-sensitive ^{1}H 2D NOESY spectra of compounds **4c** (a), **4a** (b), **4j** (c) (A, *exo-syn-anti* isomer; B, *exo-syn-syn* isomer), and **4k** (d). 1, 2, and 3 indicate the three allylic protons, H^1 being adjacent to nitrogen. The oblique arrows show the NOEs between the allylic protons and the square boxes mark the absence of cross-signals. These characteristic "absences" are also important for distinguishing between *syn* and *anti* configurations. The horizontal arrows show the NOE between *anti* proton H^3 and assigned phosphine *ortho* phenyl protons, indicating the *exo* form (see also text).

that the enantiomeric composition of the product (98:2) does not reflect the isomeric distribution of the intermediate allyl complex, indicating that the different isomers as well as the two different allyl termini should display different rates for nucleophilic attack.

The complex [Pd(η^3-1,3-diphenylallyl)((*S*)-(*R*)-**3a**)]PF_6 (**4a**), containing the 1-adamantyl ligand **3a** which affords the highest enantioselectivity, exists in solution as a single diastereomeric form, the *exo-syn-syn*. Assignment of this structure is based on the observation of NMR characteristics similar to those described above for *exo-syn-syn*-**3c**.

For the analogous complex [Pd(η^3-1,3-diphenylallyl)((*S*)-(*R*)-**3j**)]PF_6 (**4j**), containing the 9-anthryl substituent, a mixture of two isomers was observed in solution (see Chart 2). The assignment of these two structures is again based on the observation of several diagnostic NOEs, as detailed above for derivative **4c** (see Figure 3c). Thus, one of the two isomers (29%) shows the *exo-syn-syn* configuration (*syn-syn* as shown by NOEs between the terminal *anti* allyl protons and *exo* via the NOE between the central proton and protons on the anthryl group). However, the major component is now an *exo-syn-anti* isomer (71%), the *anti* configurated allyl carbon being the one cis to the N-moiety, based on intraligand NOEs between two allyl protons and the anthryl group.

Nucleophilic attack at the carbon atom trans to phosphorus should lead preferentially to the formation of the *S*-configurated product during catalysis. This is indeed what we find, and this observation thus corroborates the hypothesis that the allylic terminus trans to the phosphine behaves as the more electrophilic center. However, this observation on **4j**, taken alone, cannot conclusively exclude attack at the carbon trans to nitrogen which would also lead to the *S*-product. Nevertheless, it is worth noting that, in this case, the ratio of the two configurational isomers reflects the observed ratio of enantiomers for the product of the catalytic reaction within 1−2%. If the nucleophilic attack indeed takes place in both cases only at the carbon atom trans to phosphorus, this would imply a very similar reaction rate of the two isomers. Finally, it is important to note that on the NMR time scale, up to 60 °C, we did not observe any equilibrium between the two isomers.[16]

With these results in hand, we decided to construct a ligand

Chart 2

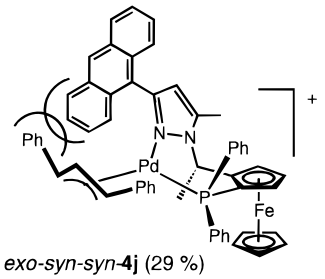

exo-syn-syn-**4j** (29 %)

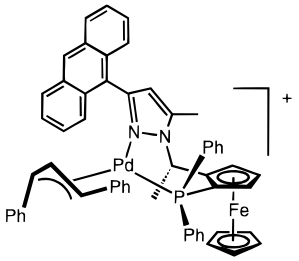

exo-syn-anti-**4j** (71 %)

which would induce the formation of an *exo-syn-anti* configurated isomer exclusively. Since the formation of this isomer seemed to be favored by the presence of a very bulky substituent at position 3 of the pyrazole, we reasoned that this could be achieved by a group larger than a 9-anthryl. Selective stabilization of the *anti* configuration in (η^3-allyl)palladium complexes based on steric repulsion has been reported previously by Åkermark, Vitagliano, and co-workers, using 2,9-disubstituted-1,10-phenanthroline ligands.[17] In our case, and for the sake of simplicity, the group exerting the necessary steric bulk should also be as symmetrical as possible. This was achieved with the 9-triptycyl substituted ligand **3k** (see Chart 3). In fact in the major component (90%) of the corresponding complex [Pd(η^3-1,3-diphenylallyl)((*R*)-(*S*)-**3k**)]PF_6 (**4k**), only one form, the *exo-syn-anti* configuration, could be identified in solution by NOESY spectroscopy (see Figure 3d). This is confirmed by (1) the usual absence of NOEs between the terminal allyl protons (*syn-anti* structure, *anti* cis to N), (2) an NOE between the central allyl proton and the terminal one trans to the phosphine, and (3) NOEs between these two protons and protons on the triptycyl fragment (*exo* form). The proximity between the allyl ligand and the triptycyl group also seems to constitute a sufficiently high barrier such that at room temperature no free rotation of the latter is observed on the NMR time scale (all protons on the triptycyl fragment are inequivalent).[18] A minor component (10%) observed in solution shows very broad signals and could not be assigned a defined structure.[19]

The X-ray crystal structure analysis of **4k** confirms the *exo-syn-anti* configuration and shows that the *anti*-configurated half

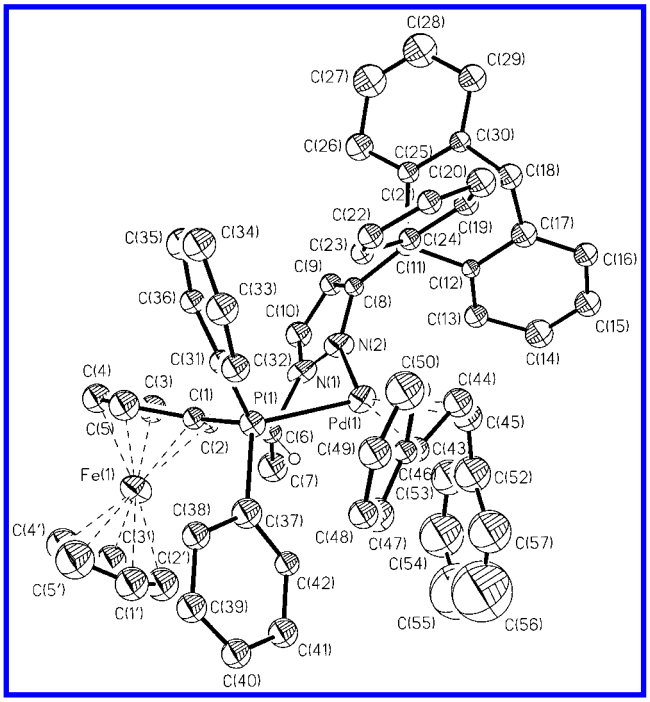

Figure 4. ORTEP view (20% ellipsoids) and atom numbering scheme for the cation (*R*)-(*S*)-**4k**.

Chart 3

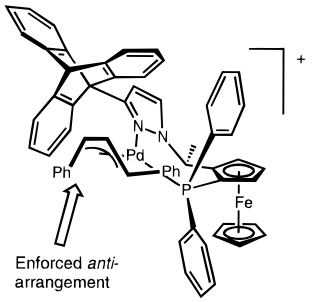

exo-syn-anti-**4k**

of the allyl ligand is nicely imbedded into one of the three cavities created by the propeller-shaped triptycyl moiety (see Figure 4; for a selection of important bond distances and angles, see Table 2). The general geometric features of the cation **4k** are very similar to those found for cation **4j** (vide supra). Thus, with respect to the rest of the molecule, the orientation of the palladium coordination plane, as defined by the atoms Pd, P, and N(2), forms angles of 108.6° and 34.5° with the allyl ligand and with the "upper" Cp ring, respectively. The *anti* arrangement of the phenyl group on C(45) is reflected by the observed torsion angle C(43)−C(44)−C(45)−C(52) of 32°, as opposed to a value of 170° for the partner angle C(45)−C(44)−C(43)−C(46) (corresponding similar absolute values of 168° and 172° were observed in complex **4c**). The only crystallographically characterized Pd-allyl complexes known in the literature containing an *anti* oriented aryl substituent involve 1,1,3-triarylallyl ligands.[20] Similarly to compound **4c**, one observes a distorsion of the allyl ligand in **4k**, such that the angles between the Pd−

(16) Such an interconversion ought to display a high activation barrier since, if operating, it could not take place via simple $\pi-\sigma-\pi$−equilibria only but probably would also require an apparent rotation of the allyl ligand. This could occur, e.g., via a dissociation of the pyrazole fragment leading to a T-shaped intermediate, followed by a rotation around the Pd−P bond and reformation of the chelate ring, as recently reported by Gogoll, Bäckvall, and co-workers for analogous systems. See: Gogoll, A.; Örnebro, J.; Grennberg, H.; Bäckvall, J.-E. *J. Am. Chem. Soc.* **1994**, *116*, 3631−3632.

(17) (a) Åkermark, B.; Hansson, S.; Vitagliano, A. *J. Am. Chem. Soc.* **1990**, *112*, 4587−4588. (b) Sjögren, M. P. T.; Hansson, S.; Norrby, P.-O.; Åkermark, B.; Cucciolito, M. E.; Vitagliano, A. *Organometallics* **1992**, *11*, 3954−3964. For related studies, see also: (c) Hansson, S.; Norrby, P.-O.; Sjögren, M. P. T.; Åkermark, B.; Cucciolito, M. E.; Giordano, F.; Vitagliano, A. *Organometallics* **1993**, *12*, 4940−4948. (d) Åkermark, B.; Zetterberg, K.; Hansson, S.; Krakenberger, B.; Vitagliano, A. *J. Organomet. Chem.* **1987**, *335*, 133−142. (e) Brown, J. M.; MacIntyre, J. E. *J. Chem. Soc., Perkin Trans. II* **1985**, 961−970. (f) Gogoll, A.; Örnebro, J.; Grennberg, H.; Bäckvall, J.-E. *J. Am. Chem. Soc.* **1994**, *116*, 3631−3632.

(18) A bipyridine system containing a triptycyl substituent has recently been described as "molecular brake", by virtue of a conformational change induced by the complexation to a metal ion that blocks the free rotation of the triptycyl fragment. See: Ross Kelly, T.; Bowyer, M. C.; Vijaya Bhaskar, K.; Bebbington, D.; Garcia, A.; Lang, F.; Kim, M. H.; Jette, M. P. *J. Am. Chem. Soc.* **1994**, *116*, 3657−3658.

(19) We presume that the minor isomer adopts a different conformation of the chelate ring, thus allowing for a slow rotation of the triptycyl moiety on the NMR time-scale.

P−N(2) plane and the two planes Pd−C(43)−C(44) and Pd−C(44)−C(45) are significantly different from one another (20.7° and 43.2°, respectively, see Figure 2b). A point worth noting about the structure of complex **4k** is the angle C(44)−C(45)−C(46) of 135.9(23)°, representing a large deviation from the expected 120°.

To our knowledge, compound **4k** is the first example of a complex with an open 1,3-disubstituted allyl ligand selectively adopting a *syn,anti* configuration that has been characterized by X-ray diffraction.

Catalytic experiments using ligand **4k** did not afford any product, even at reflux temperature in THF for days. This at first sight disappointing observation is in fact very instructive and can be rationalized as follows. The nucleophilic attack presumed to take place at the carbon atom adjacent to the triptycyl fragment is now hampered for steric reasons, presumably. Due to the *anti* arrangement of the phenyl group at that center and its position out of the allyl plane away from the metal, the trajectory of the incoming amine nucleophile is likely to be different from that for the corresponding *syn* orientation. In the former case this trajectory can be described as "from above", i.e., from a region of space where the bulky triptycyl is located. Another possible explanation relates to severe steric interactions within the Pd(0) olefin complex to be formed upon nucleophilic attack. In order to form the coordinated olefin, the allyl fragment has to slide toward the bulky triptycyl fragment, intruding even more into its cavity. This movement seems unlikely, if one considers the relatively short distance between C(45) (the electrophilic center) and the plane of the phenylene ring C(12)−C(17) of 3.51 Å observed in the crystal structure of **4k** (shortest nonbonding interatomic distance: C(45)−C(13) = 3.55 Å). Furthermore, the lack of reactivity of complex **4k** toward benzylamine also indicates that the electrophilicity of the second allylic terminus is not high enough to afford the aminated reaction product, i.e., the alternative site of attack is being "ignored" by the nucleophile. This very fact constitutes a further indirect piece of evidence that in the present Pd(allyl) system containing P,N-ligands, the nucleophile benzylamine attacks preferentially or probably even exclusively at the carbon atom in trans position with respect to the phosphine.

Conclusions

An explanation of the pronounced site-selectivity observed can be based on a simple ground-state argument. The crucial carbon atom is subjected to a much higher trans influence than the one trans to the pyrazole nitrogen, as reflected by both the longer bond distance to palladium (see Table 2) and by the larger deshielding observed in ^{13}C NMR spectra (see Table 3). These characteristics render this carbon atom more electrophilic than its companion trans to nitrogen. The simple ground state argument will of course have validity only for an early transition state of the nucleophilic attack (Hammond postulate, see Chart 4). However, in the course of C−N bond formation an important distorsion of the allyl ligand should take place. Specifically, the latter should rotate around the Pd-allyl axis in order for the developing double bond to move into coplanarity with the Pd−P−N(2) plane, a situation rather consistent with a late (product-like) transition state. *Precisely this distorsion is observed* in the crystal structures described above.[21] Thus, in the ground-state of the intermediates examined, two important structural features indicate and explain the very high site-

Chart 4

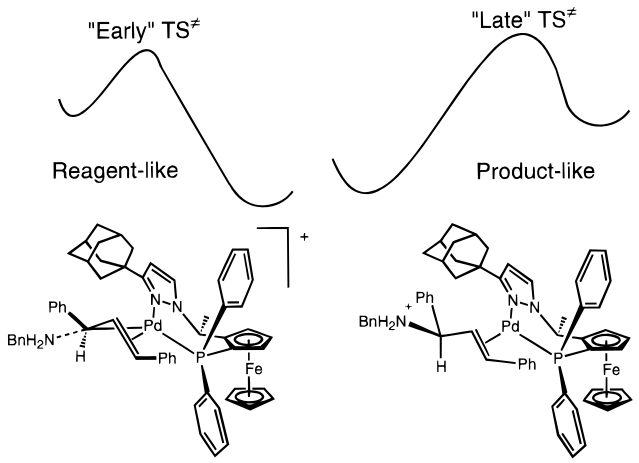

preference for nucleophilic attack and strongly indicate that an early (reagent-like) transition state is involved: (1) the carbon atom trans to phosphorus is electronically set up to be more electrophilic, and (2) the other two carbon atoms are already "prepared" to lie in the main coordination plane of the Pd(0) olefin complex forming upon nucleophilic attack. From these considerations and from the fact that complex **4a** exists as single *exo-syn-syn* isomer, one can draw the following conclusion. The observed enantiomer ratio of the amination product **2** (>ca. 200:1) in the reaction involving intermediate **4a** corresponds to the ratio of the rates for nucleophilic attacks at the carbon trans to phosphorus and trans to nitrogen, respectively. In other words, the activation barrier for C−N bond formation trans to phosphorus must be at least ca. 3 kcal·mol^{-1} lower than for the analogous process trans to nitrogen.

Finally, the virtual lack of reactivity of the allylic carbon trans to nitrogen could be explained by the fact that the necessary distorsion of the Pd-allyl moiety should take place in the opposite sense, thus requiring a more drastic rearrangement in the transition state, and hence not obeying the principle of least motion.[22] Furthermore, if this were to be the case, probable unfavorable steric interactions would develop during the transition state. For instance, the evolving pyramidalization of the carbon atom being attacked by benzylamine would "push back" the allylic phenyl group toward the phosphine phenyls, a region of the molecule where not sufficient space appears to be available for this movement.

In order to shed more and conclusive light on these subtle mechanistic aspects ab initio molecular dynamics calculations (projector augmented wave method) on this system are currently being carried out.[23]

Experimental Section

General Considerations. All reactions with air- or moisture-sensitive materials were carried out under an argon or nitrogen atmosphere using standard Schlenk techniques. Freshly distilled, dry, and oxygen-free solvents were used throughout. 1D- and 2D-NMR experiments were carried out using a Bruker AMX 500 spectrometer on 0.02 mmol samples in $CDCl_3$ or THF-d_8. Standard pulse sequences were employed for ^1H-2D-NOESY,[24] $^{13}C-^1H$-,[25] and $^{31}P-^1H$-correlation studies.[26] The latter two types of experiments were used for resonance

(20) Farrar and Payne reported the complex [Pd(*S,S*-chiraphos)(η^3-(xylyl)$_2$CCHCHPh)]BPh_4 , see: Farrar, D. H.; Payne, N. C. *J. Am. Chem. Soc.* **1985**, *107*, 2054−2058, and we described more recently the compound [Pd(sparteine)(η^3-(Ph)$_2$CCHCHPh)][CF_3SO_3], see: Togni, A.; Rihs, G.; Pregosin, P. S.; Ammann, C. *Helv. Chim. Acta* **1990**, *73*, 723−732.

(21) This important aspect has been brought to our attention by Dr. J. M. Brown, Oxford University, who observed similar distorsions for the system reported in ref 3k.

(22) For a review of this principle, see: Hine, J. *Adv. Phys. Org. Chem.* **1977**, *15*, 1−61.

(23) Blöchl, P. E.; Togni, A., manuscript in preparation.

(24) Jeener, J.; Meier, B. H.; Bachmann, P.; Ernst, R. R. *J. Chem. Phys.* **1979**, *71*, 4546−4553.

assignment purposes. The phase-sensitive NOESY experiments used mixing times of 0.8 s. IR spectra of KBr pellets were recorded on a Perkin-Elmer Paragon 1000 FT spectrometer. Ligands **3** were prepared as reported from our laboratory.[7b] Catalytic experiments and the assignment of the absolute configuration of the product **2** were carried out following a reported procedure.[6a] Enantiomeric excesses were determined by HPLC using a Daicel Chiralcel OJ column and eluting with an hexane/*i*-PrOH mixture (87:13 v/v; 0.5 mL/min; $T = 25$ °C; retention times: (*S*)-**2** 16.8 min, (*R*)-**2** 19.5 min)). Elemental analyses as well as mass spectra were performed by the "Mikroelementar-analytisches Laboratorium der ETH".

[Pd(η^3-PhCHCHCHPh)((*R*)-(*S*)-3a)][PF_6] (4a). To a solution of ligand (*R*)-(*S*)-**3a** (100 mg, 0.167 mmol) in acetone (10 mL) was added [Pd(η^3-PhCHCHCHPh)(μ-Cl)]$_2$ (50.9 mg, 0.076 mmol). After the solution had turned clear again, solid $TlPF_6$ (53.1 mg, 0.152 mmol) was added, and stirring continued for 1 h. The suspension was filtered over Celite, the solvent was evaporated in vacuo except for a few milliliters, and the product precipitated with hexane. Repeated filtration over Celite, followed by recrystallization from dichloromethane/hexane yielded compound **4a** as an amorphous solid (155 mg, 98%). An analytical sample was dried under vacuo: IR (cm^{-1}) 3056, 2903, 2849, 1546, 1511, 1490, 1448, 1434, 1356, 1304, 1241, 1204, 1162, 1002, 842 (PF_6), 755, 696, 558; MS (FAB^+) *m/z* 1941 ($M_2PF_6^+$), 1042 (($MPF_6 - H)^+$), 897 (M^+, 100%), 704 (M^+ − PhCHCHCHPh), 307, 154. Anal. Calcd for $C_{52}H_{52}F_6FeN_2P_2Pd$: C, 59.87; H, 5.02; N, 2.69. Found: C, 60.12; H, 5.53; N, 2.57.

[Pd(η^3-PhCHCHCHPh)((*S*)-(*R*)-3c)][PF_6] (4c). To a solution of ligand (*S*)-(*R*)-**3c** (85 mg, 0.15 mmol) in acetone (15 mL) was added [Pd(η^3-PhCHCHCHPh)(μ-Cl)]$_2$ (45 mg, 0.067 mmol). After the solution had turned clear again, solid $TlPF_6$ (47 mg, 0.135 mmol) was added, and stirring continued for 1 h. Workup as detailed above, followed by recrystallization from hexane/diethyl ether yielded 110 mg (82%) of compound **4c** as orange needles suitable for X-ray, containing 1 equiv of Et_2O. An analytical sample was dried in vacuo, thus releasing the co-crystallized Et_2O; IR (cm^{-1}) 1548, 1482, 1437, 1372, 1321, 1245, 1163, 1101, 1045, 842 (PF_6), 756, 696, 558; MS (FAB^+) *m/z* 853 (M^+, 100%), 732 (M^+ − FeCp), 660 (M^+ − PhCHCHCHPh), 502 (660−Hpz), 369, 291, 212, 154. Anal. Calcd for $C_{49}H_{44}F_6FeN_2P_2$-Pd: C, 58.91; H, 4.44; N, 2.80. Found: C, 58.79; H, 4.42; N, 2.87.

[Pd(η^3-PhCHCHCHPh)((*S*)-(*R*)-3j)][BF_4] (4j). To a solution of ligand (*S*)-(*R*)-**3j** (50 mg, 0.076 mmol) in dichloromethane (10 mL) was added [Pd(η^3-PhCHCHCHPh)(μ-Cl)]$_2$ (24 mg, 0.036 mmol). After the solution had turned clear again, $AgBF_4$ (14 mg, 0.072 mmol), solved in 5 mL of methanol, was added and stirring continued for 1 h. Workup as detailed above, followed by recrystallization from dichloromethane/hexane yielded 57 mg (76%) of compound **4j** as a bright yellow powder: IR (cm^{-1}) 1654, 1636, 1560, 1541, 1490, 1458, 1437, 1386, 1312, 1161, 1084, 1061 (BF_4), 831, 744, 697, 534; MS (FAB^+) *m/z* 953 (M^+), 760 (M^+−PhCHCHCHPh), 327, 281, 207, 147, 73 (100%). Anal. Calcd for $C_{57}H_{48}BF_4FeN_2PPd\cdot 0.5\ CH_2Cl_2$: C, 63.74; H, 4.56; N, 2.58. Found: C, 63.67; H, 4.74; N, 2.84.

[Pd(η^3-PhCHCHCHPh)((*R*)-(*S*)-3k)][PF_6] (4k). To a solution of ligand (*R*)-(*S*)-**3k** (100 mg, 0.14 mmol) in acetone (15 mL) was added [Pd(η^3-PhCHCHCHPh)(μ-Cl)]$_2$ (42.5 mg, 0.063 mmol). After the solution had turned clear again, solid $TlPF_6$ (44 mg, 0.127 mmol) was added and stirring continued for 1 h. Workup as detailed above, followed by recrystallization from acetone/hexane yielded 118 mg (80%) of compound **4k** as dark orange crystals, containing 1 equiv of acetone: IR (cm^{-1}) 3057, 1623, 1512, 1490, 1457, 1242, 1163, 1097, 1002, 842 (PF_6), 751, 697, 633, 558; MS (FAB^+) *m/z* 1015 (M^+), 822 (M^+ − PhCHCHCHPh, 100%), 716 (822−Pd), 651 (716−cp), 502 (822−Hpz), 397 (716−Hpz), 331 (397−cp), 289, 212 (397−PPh_2), 154. Anal. Calcd for $C_{62}H_{50}F_6FeN_2P_2Pd\cdot C_3H_6O$: C, 64.03; H, 4.63; N, 2.30. Found: C, 63.82; H, 4.93; N, 2.37.

X-Ray Crystallographic Study of (*S*)-(*R*)-4c and (*R*)-(*S*)-4k. Crystallographic and data collection parameters are provided as supporting information. Data were measured with variable scan speed to ensure constant statistical precision on the collected intensities. One standard reflection was measured every 120 reflections; no significant variation was detected. However, because of their fast decay when taken out of the mother liquor (loss of enclosed solvent molecules), crystals of **4k** were embedded in silicon grease and a selected one mounted in a glass capillary. Scan speed was raised to prevent crystal decay during data collection. Because of the silicon mantle, outer reflections were generally weak, and no reflections beyond $2\theta = 40°$ could be detected. For both compounds no correction for absorption was applied. The structures were solved either by Patterson (**4c**) or direct (**4k**) methods and refined by full-matrix least squares using anisotropic displacement parameters for all non-hydrogen atoms (**4c**) and for both non-hydrogen and non-carbon atoms (**4k**), respectively. Hydrogen atoms were refined in their idealized position (riding model with fixed isotropic $U = 0.080$ Å^2). Because of the relatively poor quality of the data of **4k**, all carbon rings as well as the PF_6^- counteranion were refined as rigid groups. Solvent molecules found in the crystal packing of both **4c** and **4k** were highly disordered and could not be unequivocally assigned. For **4k** in particular, best results were obtained by assuming the presence of three molecules of hexane, one molecule of acetone, and one of water, per one equiv of **4k**, and by refining them without constraints. All calculations were carried out by using the Siemens SHELXTL PLUS system.

Acknowledgment. This research was supported by LONZA Ltd. (Ph.D. grant to U.B.).

Supporting Information Available: Tables of crystal data and refinement details, atomic coordinates, complete listing of bond distances and angles, tables of anisotropic displacement coefficients for non-carbon atoms, and coordinates of hydrogen atoms for compounds **(*S*)-(*R*)-4c** and **(*R*)-(*S*)-4k**, a section of the phase sensitive ^{1}H-2D-NOESY spectrum of compound **4c**, showing the exchange occurring between the *exo-syn-syn* and the *endo-syn-anti* isomers, and 500 MHz ^{1}H NMR spectra of compounds **4a**, **4c**, **4j**, and **4k** (28 pages). This material is contained in many libraries on microfiche, immediately follows this article in the microfilm version of the journal, can be ordered from the ACS, and can be downloaded from the Internet; see any current masthead page for ordering information and Internet access instructions.

JA953031G

(25) Summers, M. F.; Marzilli, L. G.; Bax, A. *J. Am. Chem. Soc.* **1986**, *108*, 4285−4294.

(26) Sklenár, V.; Miyashiro, H.; Zon, G.; Miles, H. T.; Bax. A. *FEBS Lett.* **1986**, *208*, 94−98.